# Shedding light on Dark Matter Using Extended Higgs Sectors

Juhi Dutta

based on

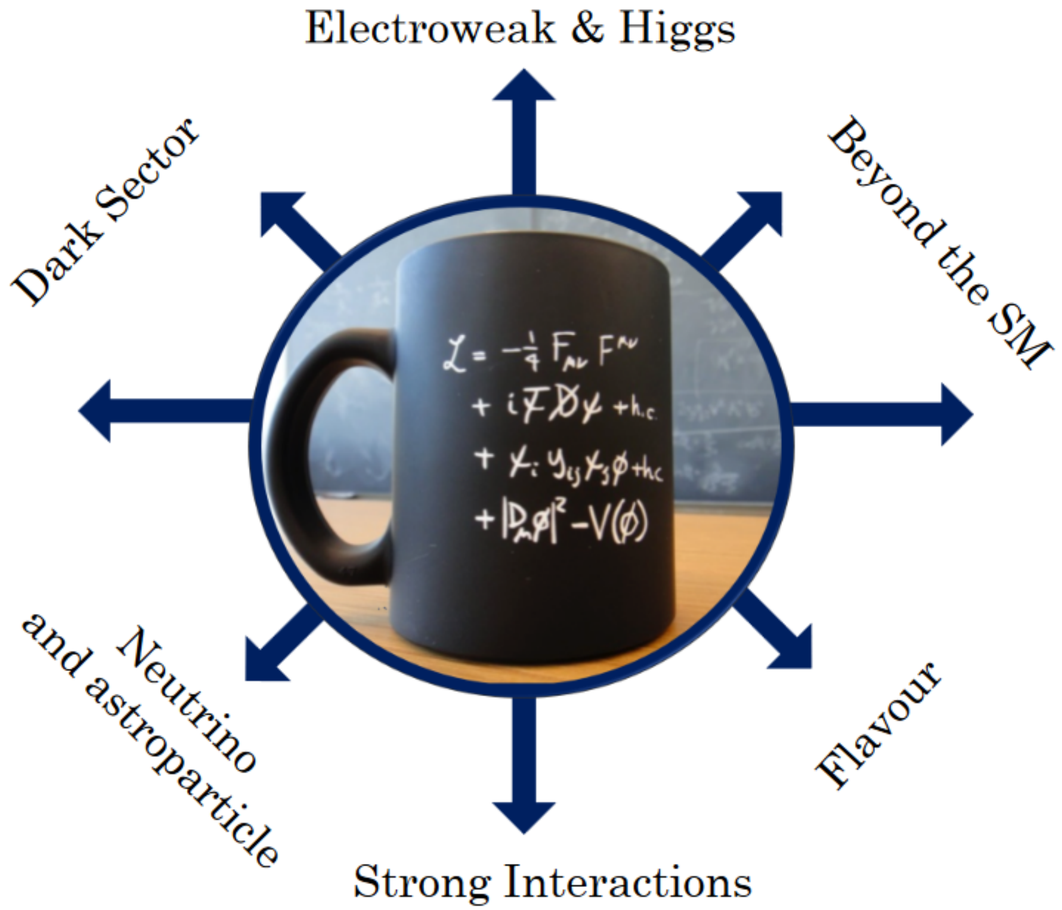
***Eur.Phys.J.C 84 (2024) 9, 926, Eur.Phys.J.C 86 (2026) 4, 384, Eur.Phys.J.Plus 140 (2025) 1, 87***

*with J. Lahiri, C. Li, G. Moortgat-Pick, M.Schreiber, S.F.Tabira, J.A. Ziegler*

***The International Workshop on Future Linear Colliders 2026 (LCWS2026), KEK, Japan***

November 12, 2026

# Synergy of Higgs to New Physics?




CERN

# Extended Higgs Sectors

Dark Matter

Higgs Phenomenology

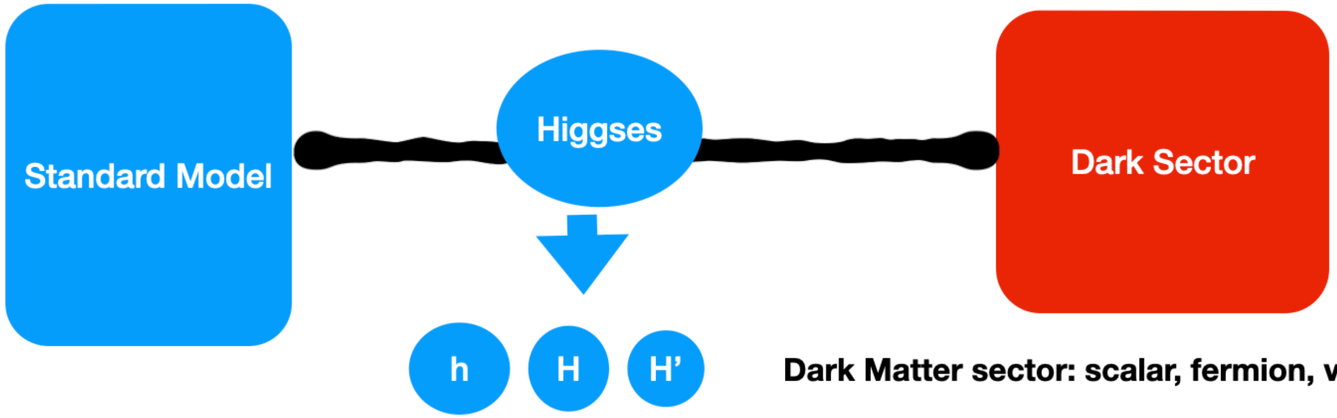
Scalar excesses, e.g, “~95 GeV” excess

Inflation

Baryogenesis

Leptogenesis

Gravitational Waves




Dark Matter sector: scalar, fermion, vector

Eg. in
2HDM + complex singlet scalar (2HDMS) with DM stabilized by a $Z_2'$ symmetry.

Baum, et.al, *JHEP*12(2018)044

Dutta et.al, Eur.Phys.J.Plus 140 (2025) 1, 87, 2504.14529,

*Eur.Phys.J.C 84 (2024) 9, 926, ongoing works.*

S.Heinemeyer et.al, Phys. Rev. D 106 (2022), no. 7 075003

*Matlis et.al, JCAP 07 (2024) 007*

*Biekotter,et.al 2509.01682, JHEP 10 (2022) 126*

Drozd et.al JHEP11 (2014) 105, Dey et.al JHEP 09 (2019) 004

# Extended Higgs Portal Models:
# 2HDM + complex singlet scalar (2HDMS)

- Consider a softly broken $Z_2$ (to avoid FCNC) symmetric Type II 2HDM augmented with a complex scalar singlet S, with the imaginary component stabilized under $Z_2'$.

- Depending on the singlet vev $v_S$, the model can accommodate single or multicomponent dark matter candidates.

- The scalar potential $V_{2HDMS} = V_{2HDM} + V_S$,

| Model | $u_R^i$ | $d_R^i$ | $e_R^i$ |
|---|---|---|---|
| Type I | $\Phi_2$ | $\Phi_2$ | $\Phi_2$ |
| Type II | $\Phi_2$ | $\Phi_1$ | $\Phi_1$ |
| Lepton-specific | $\Phi_2$ | $\Phi_2$ | $\Phi_1$ |
| Flipped | $\Phi_2$ | $\Phi_1$ | $\Phi_2$ |

$$\Phi_i = \begin{pmatrix} \phi_i^{\pm} \\ \frac{1}{\sqrt{2}}(v_i + h_i + ia_i) \end{pmatrix}, \quad i = 1, 2,$$

$$S = \frac{1}{\sqrt{2}}(v_S + h_S + ia_S)$$

$$V_{2HDM} = m_{11}^2\Phi_1^\dagger\Phi_1 + m_{22}^2\Phi_2^\dagger\Phi_2 - (m_{12}^2\Phi_1^\dagger\Phi_2 + h.c) + \frac{\lambda_1}{2}(\Phi_1^\dagger\Phi_1)^2 + \frac{\lambda_2}{2}(\Phi_2^\dagger\Phi_2)^2 + \lambda_3(\Phi_1^\dagger\Phi_1)(\Phi_2^\dagger\Phi_2) + \frac{\lambda_4}{2}(\Phi_1^\dagger\Phi_2)(\Phi_2^\dagger\Phi_1) + \frac{\lambda_5}{2}(\Phi_1^\dagger\Phi_2)^2 + h.c,$$

$$V_S = m_S^2(S^\dagger S) + \frac{m_S^{2'}}{2}(S^2 + h.c) + \frac{\lambda_1''}{24}(S^4 + h.c) + \frac{\lambda_2''}{6}(S^2(S^\dagger S) + h.c) + \frac{\lambda_3''}{4}(S^\dagger S)^4 + \lambda_1' S^\dagger S\Phi_1^\dagger\Phi_1 + \lambda_2' S^\dagger S\Phi_2^\dagger\Phi_2 + S^2(\lambda_4'\Phi_1^\dagger\Phi_1 + \lambda_5'\Phi_2^\dagger\Phi_2) + h.c.$$

**Baum, et.al, *JHEP*12(2018)044**

# Key Points

**Particle content:**

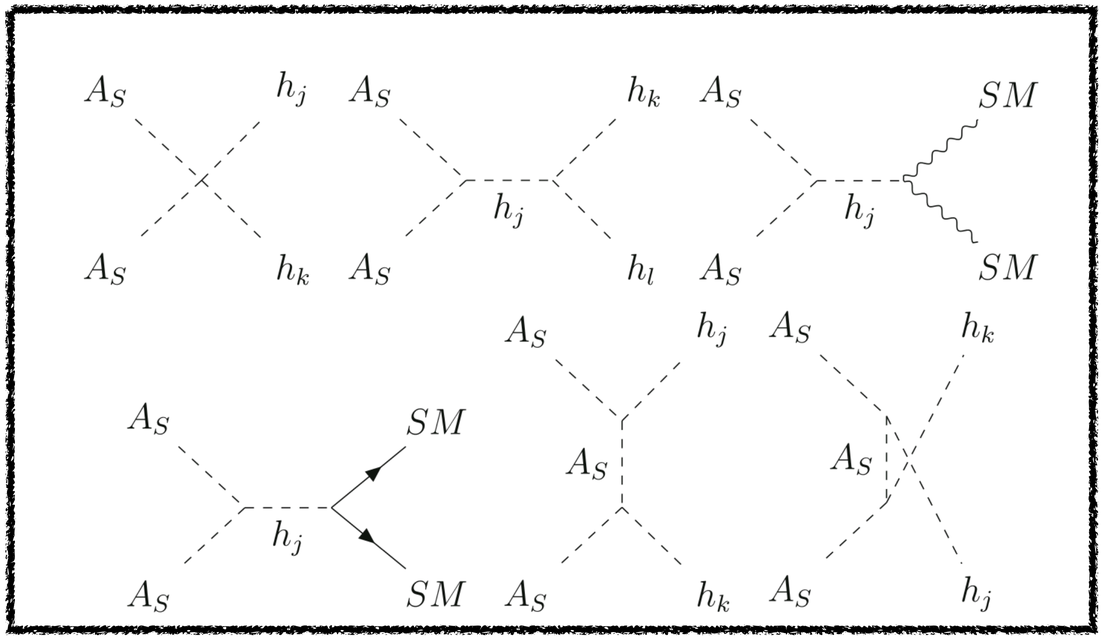
$$h_1, h_2, h_3, A, H^{\pm}, A_S$$

**Scalar Mediators** **DM**

**Dark Matter mass:**

$$m^2_{A_S} = \frac{\partial^2 V}{\partial A_S^\dagger \partial A_S}\Big|_{\substack{\Phi_1=\langle\Phi_1\rangle \\ \Phi_2=\langle\Phi_2\rangle \\ S=\langle S\rangle}}$$

$$= -(2m'^2_S + v_S^2(\frac{\lambda''_1}{3} + \frac{\lambda''_2}{3}) + 2(\lambda'_4 v_1^2 + \lambda'_5 v_2^2))$$




**Free parameters:**

$$m_{h_1}, m_{h_2}, m_{h_3}, m_A, m_{H^\pm}, m_{A_S}, , \tan\beta, v_S, \tilde{\mu}^2, \alpha_1, \alpha_2, \alpha_3$$

$$\lambda'_{14} = \lambda'_1 - 2\lambda'_4, \lambda'_{25} = \lambda'_2 - 2\lambda'_5, \lambda''_{13} = \lambda''_1 - \lambda''_3,$$

**Portal Couplings to Higgs sector**

**Trilinear and Quartic Couplings of DM to Higgs Bosons:**

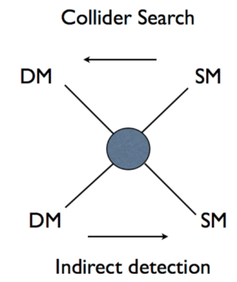
$$\frac{\lambda_{h_j A_S A_S}}{v} = -i[\lambda'_{14} c_\beta R_{j1} + \lambda'_{25} s_\beta R_{j2} - \frac{v_S}{2v}\lambda''_{13} R_{j3}]$$

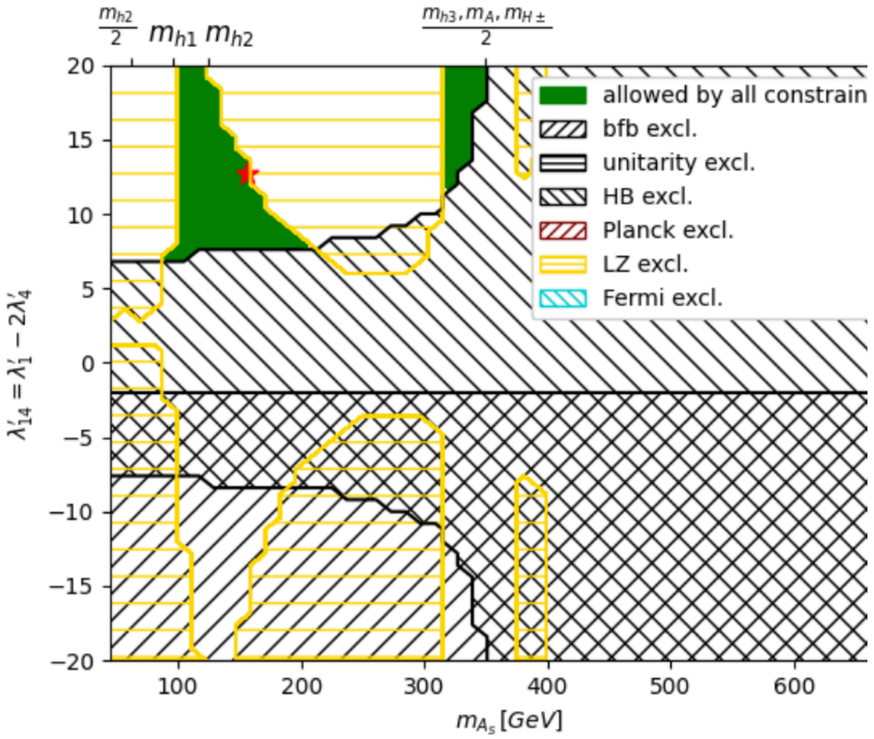
$$\lambda_{h_j h_k A_S A_S} = -i[\lambda'_{14} R_{j1} R_{k1} + \lambda'_{25} R_{j2} R_{k2} - \frac{1}{2}\lambda''_{13} R_{j3} R_{k3}],$$

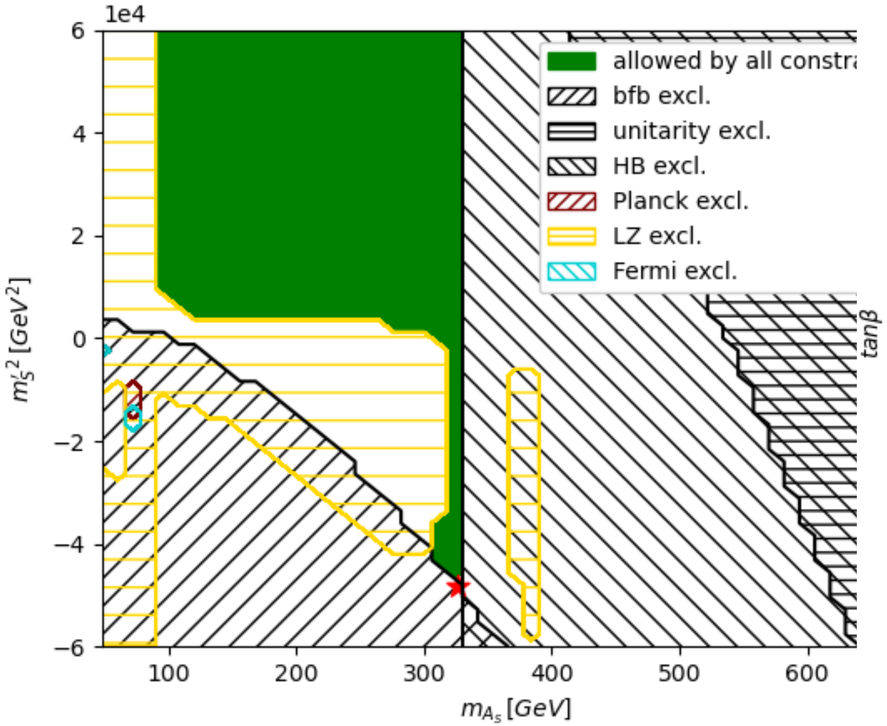
**Connection to colliders via invisible decays of SM and BSM Higgs bosons.**

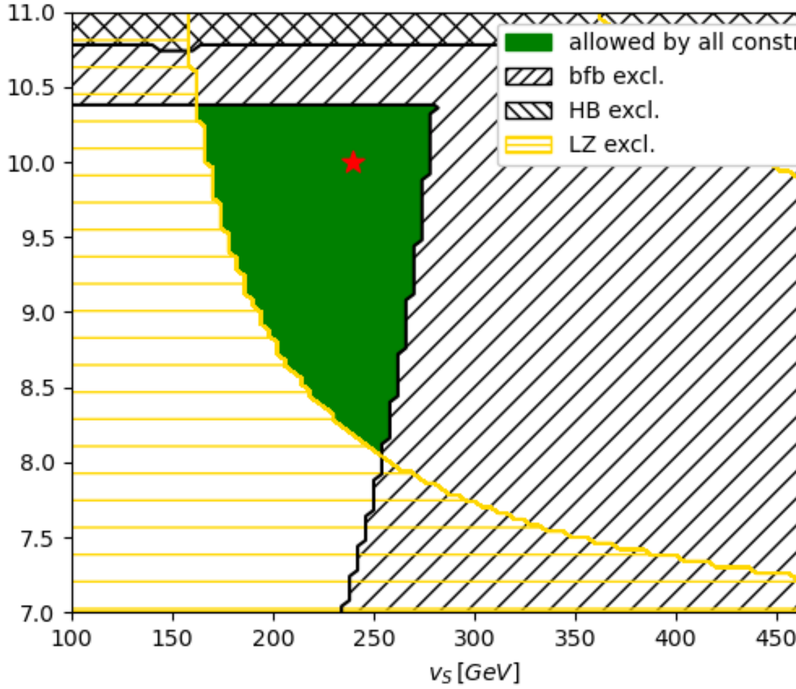
*Dutta, et.al, 2504.14529*

# Extended Higgs sectors portal to Dark Matter




**PU, BFB, B physics constraints**

**Higgs Bounds**

**SM Higgs Signal Strengths**

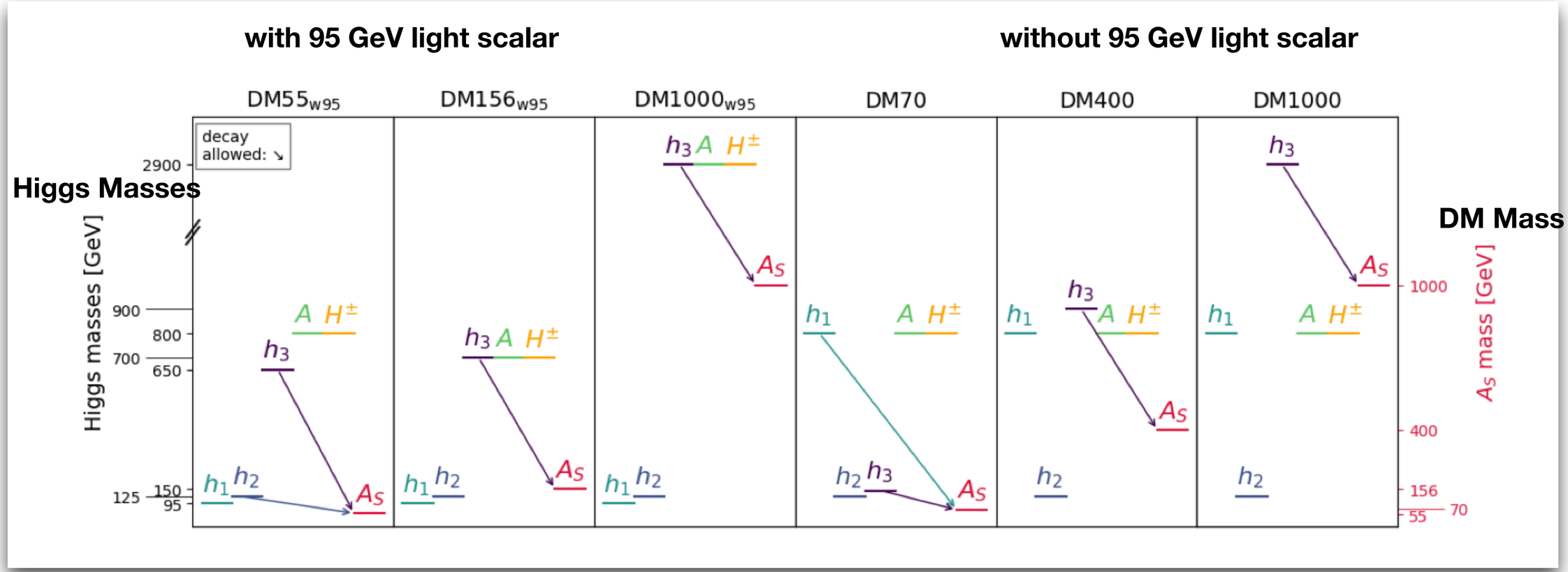
**Relic Density**

**SI cross-section**

**ID cross-section**

**Allowed Parameter Space subject to theory and experimental constraints.**

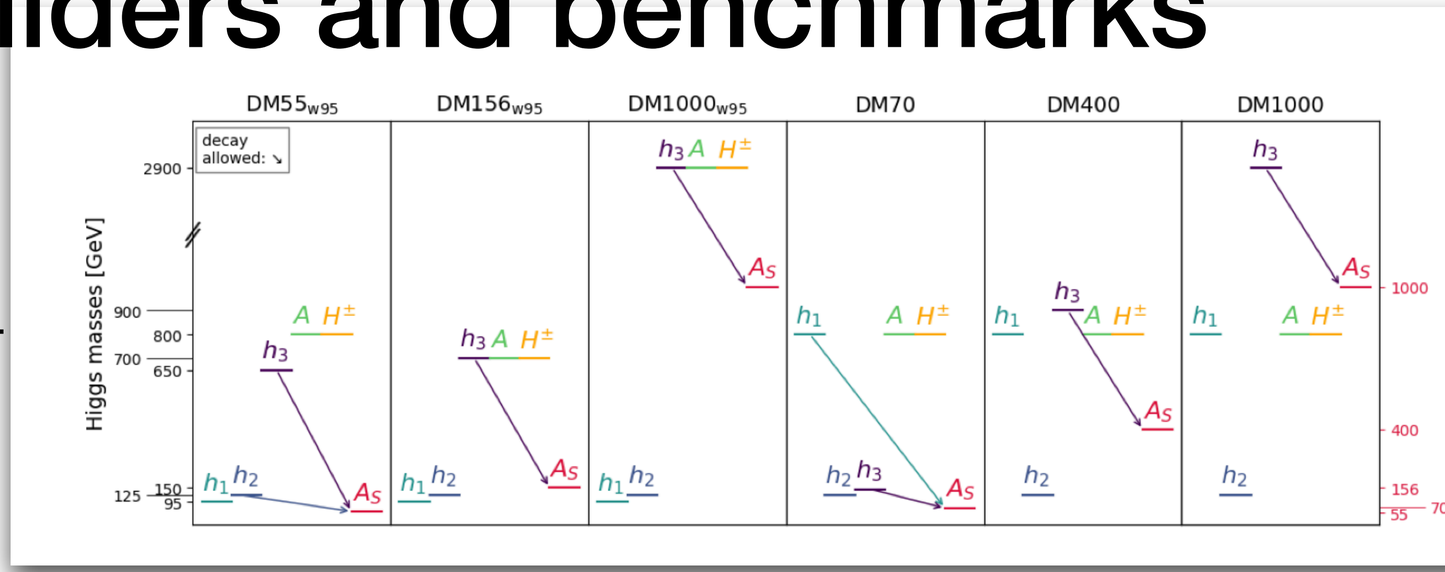
# Representative Benchmarks




| | $m_{A_S}$ (GeV) | $\tan\beta$ | $\Omega h^2$ | $BR(h_1 \to A_S A_S)$ | $BR(h_2 \to A_S A_S)$ | $BR(h_3 \to A_S A_S)$ |
|---|---|---|---|---|---|---|
| **DM55$_{\mathbf{w95}}$** | 55 | 2 | 0.11 | - | 0.0199 | $3.81 \cdot 10^{-9}$ |
| **DM156$_{\mathbf{w95}}$** | 156 | 6.6 | $1.61 \cdot 10^{-4}$ | - | - | 0.692 |
| **DM1000$_{\mathbf{w95}}$** | 1000 | 5 | 0.111 | - | - | 0.0360 |
| **DM70** | 70 | 1.37 | 0.113 | $1.80 \cdot 10^{-4}$ | - | 0.999 |
| **DM400** | 400 | 2.13 | 0.106 | - | - | 0.822 |
| **DM1000** | 1000 | 1.34 | 0.117 | - | - | 0.00514 |

# Connection to colliders and benchmarks

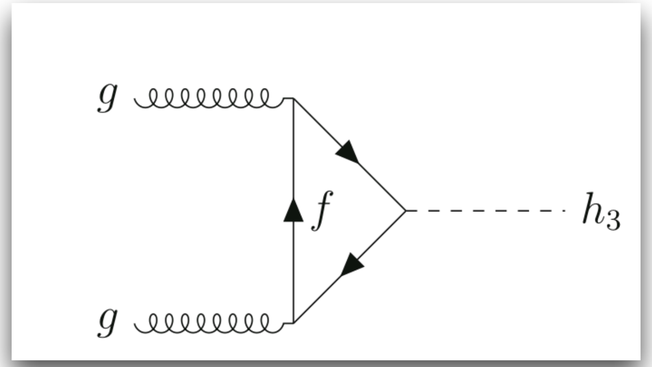
- DM invisible to colliders.
- Typical signals: SM particles + Missing energy.



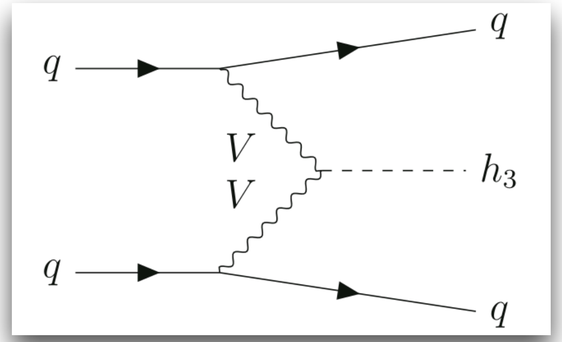

| | $m_{A_S}$ (GeV) | $\tan\beta$ | $\Omega h^2$ | $BR(h_1 \to A_S A_S)$ | $BR(h_2 \to A_S A_S)$ | $BR(h_3 \to A_S A_S)$ |
|---|---|---|---|---|---|---|
| **DM55$_{\mathbf{w95}}$** | 55 | 2 | 0.11 | - | 0.0199 | $3.81 \cdot 10^{-9}$ |
| **DM156$_{\mathbf{w95}}$** | 156 | 6.6 | $1.61 \cdot 10^{-4}$ | - | - | 0.692 |
| **DM1000$_{\mathbf{w95}}$** | 1000 | 5 | 0.111 | - | - | 0.0360 |
| **DM70** | 70 | 1.37 | 0.113 | $1.80 \cdot 10^{-4}$ | - | 0.999 |
| **DM400** | 400 | 2.13 | 0.106 | - | - | 0.822 |
| **DM1000** | 1000 | 1.34 | 0.117 | - | - | 0.00514 |

- Benchmarks chosen with thermal relic and underabundant cases satisfying all theoretical and experimental constraints.
- Potential signals at high luminosity LHC, e+e- colliders as well as muon colliders.

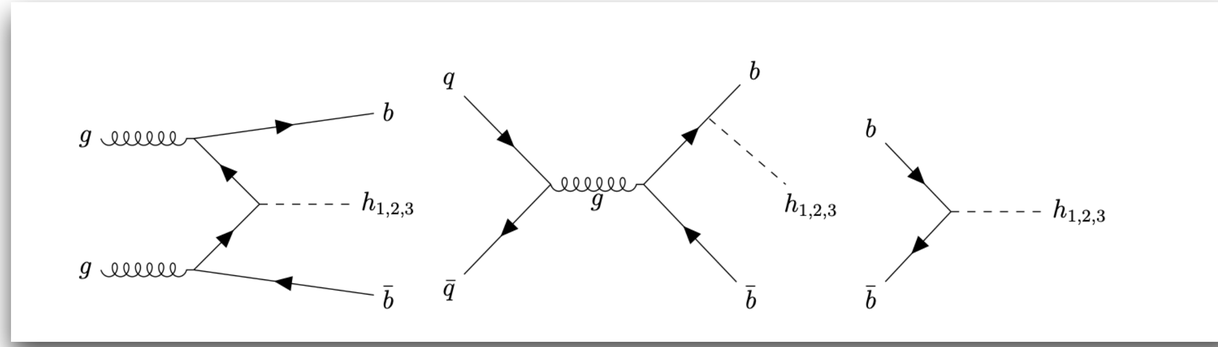
# Signals at HL-LHC




Gluon Fusion (GGF)




Vector Boson Fusion (VBF)



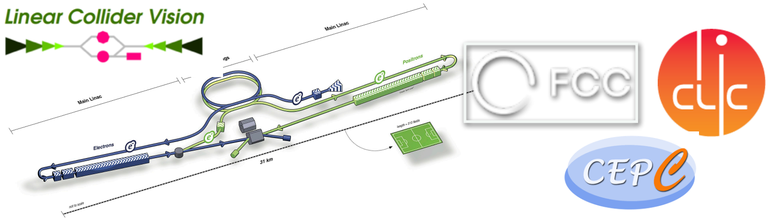

Associated bbH production for heavy Higgses (BBH)

- Signals: Mono-jet + Missing energy, Di-jet + Missing Energy, 2b jets + Missing energy

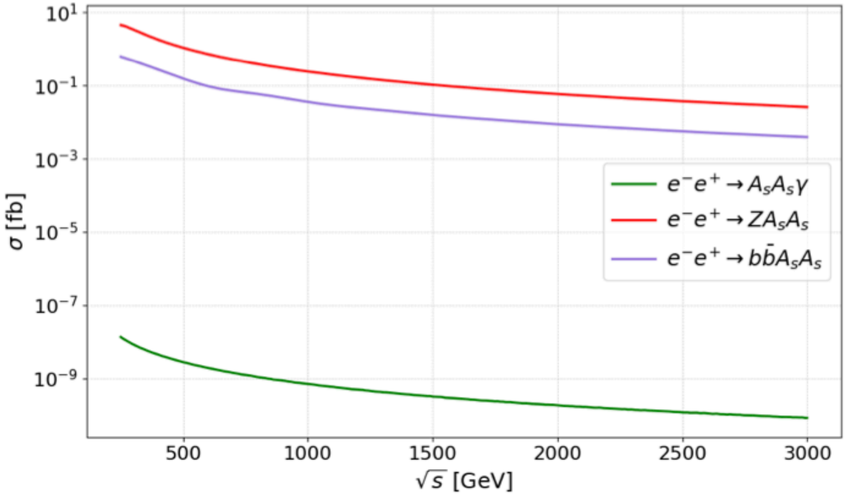
- Hints of new physics ~2$\sigma$ by the end of high luminosity LHC at 14 TeV and 3000 fb$^{-1}$.

- **Lepton colliders could play a crucial role here to uncover these scenarios with better precision and cleaner environment.**

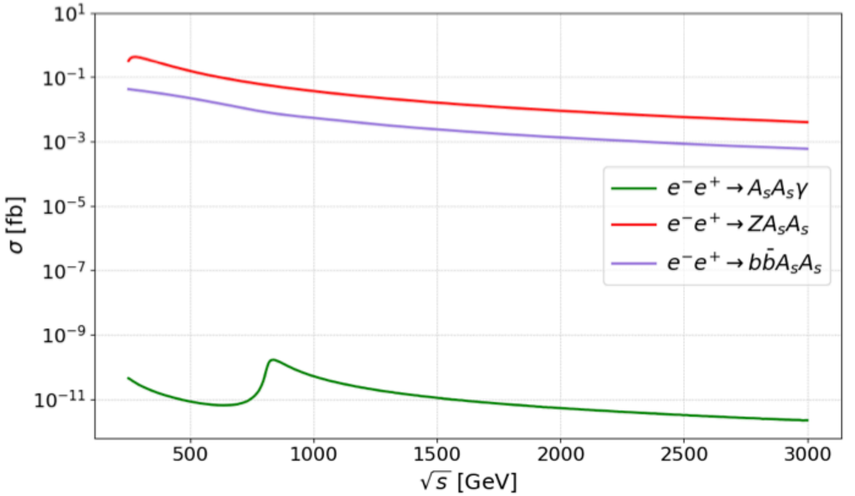
# Relevant processes at e+e- colliders



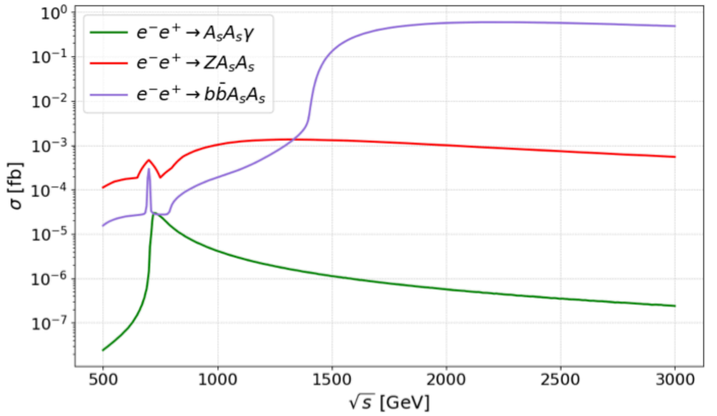

- Leading signal for light DM benchmarks Mono-Z + MET as in **DM55** and **DM70**.
- For heavier DM, **associated bbH** production channels takes over as in **DM156**.




(a) $\mathbf{DM55_{w95}}$



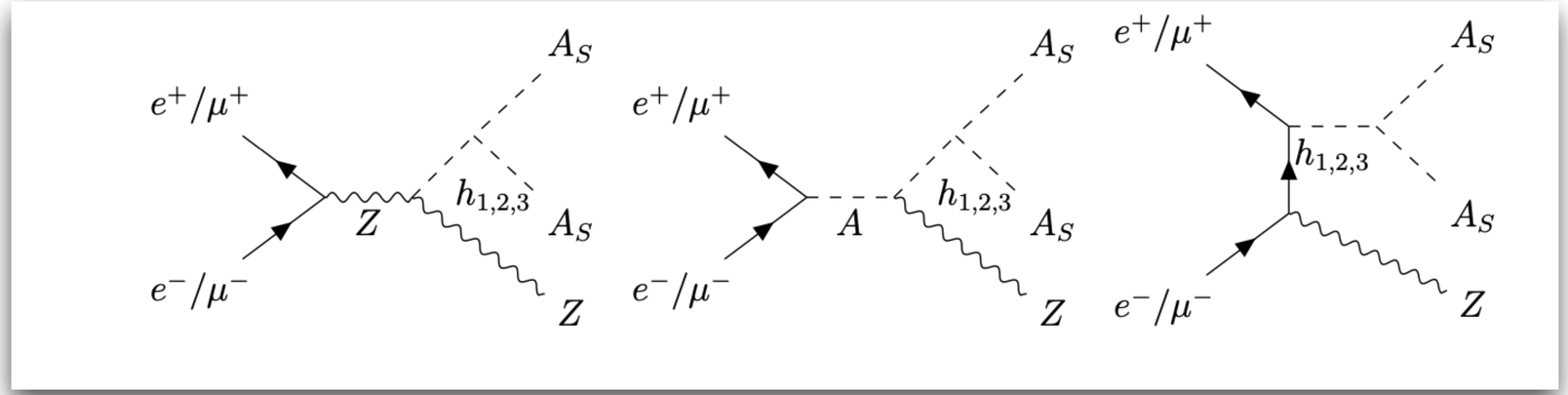

(b) $\mathbf{DM70}$




(c) $\mathbf{DM156_{w95}}$

# Signals at $e^+e^-$ colliders

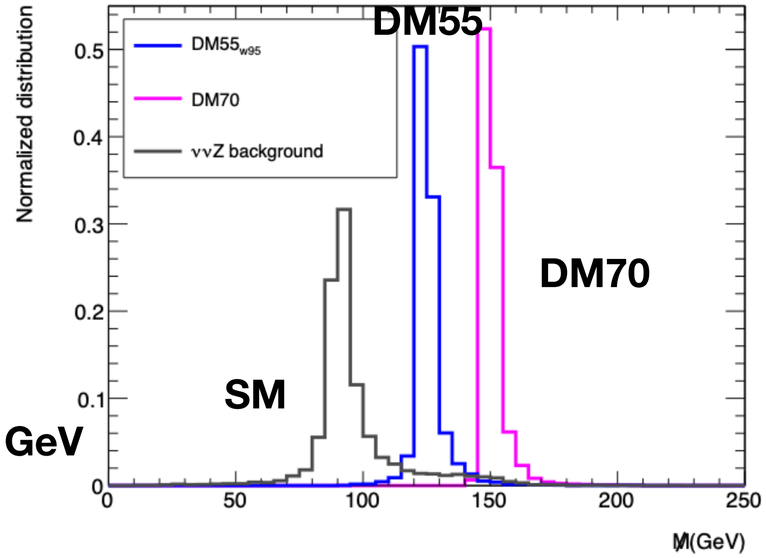
**Mono-Z + Missing Energy**

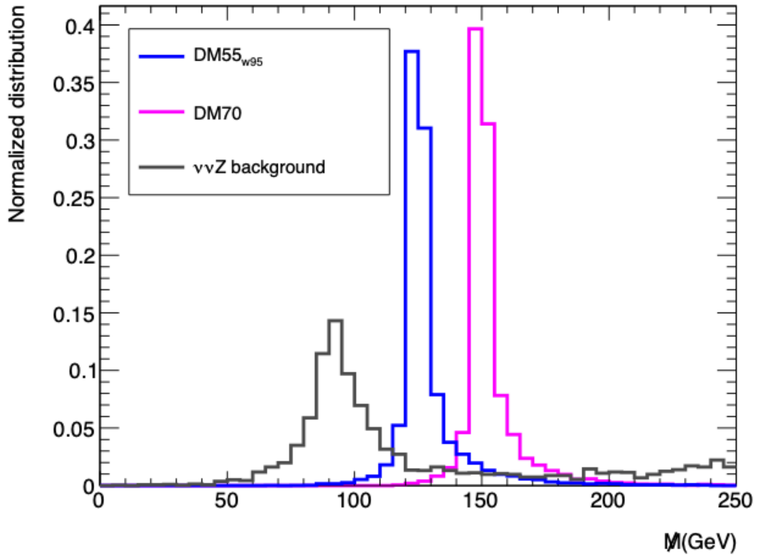



| Benchmark | Production cross-section (fb) | | |
|---|---|---|---|
| | at $\sqrt{s} = 250$ GeV | at $\sqrt{s} = 500$ GeV | at $\sqrt{s} = 1$ TeV |
| **DM55$_{\mathbf{w95}}$** | 4.42 | 1.1 | 0.24 |
| **DM70** | 0.33 | 0.15 | 0.035 |
| $\nu\bar{\nu}Z$ background | 503 | 491 | 950 |

**Signal Background Production Cross sections at various center of mass energies at an unpolarised e+e- collider experiment.**

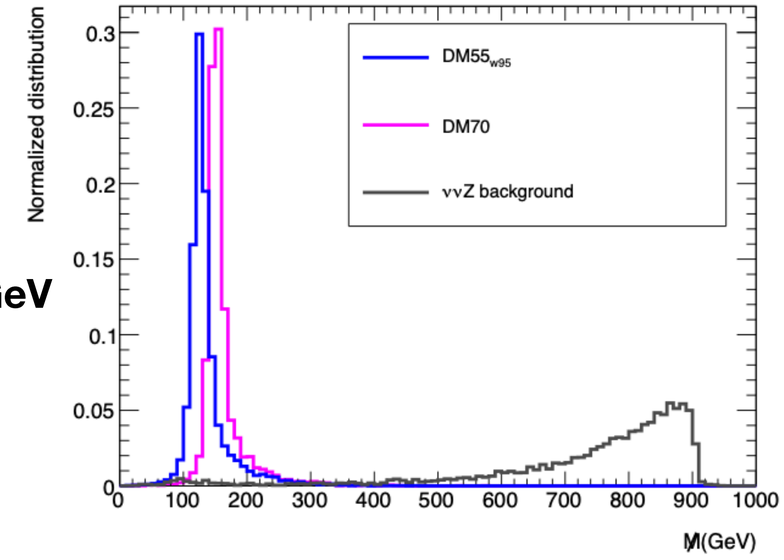
$\sqrt{s} = 250$ **GeV**




$\sqrt{s} = 500$ **GeV**

$\sqrt{s} = 1000$ **GeV**




**Missing Mass** $\not{M}^2 = (p_{in} - p_{out})^2$

**Powerful discriminator between signal and background.**

# Results

**Light Dark Matter mostly sensitive via mono-Z + missing energy final state at a e+e- collider at 250 GeV.**

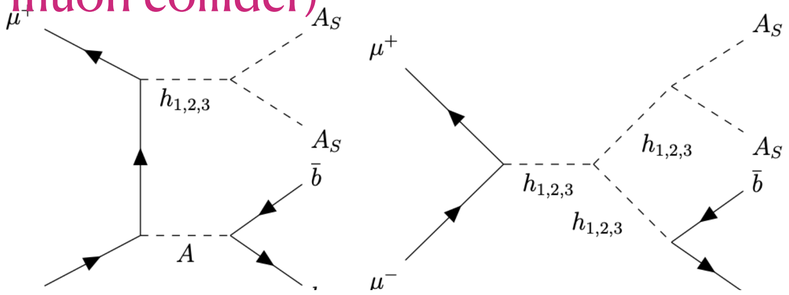
| Benchmark | $\sqrt{s}$ | Cut | Significance |
|---|---|---|---|
| $\mathbf{DM55_{w95}}$ | 250 GeV | $\not{M} > 100$ GeV | $11\sigma$ $(1ab^{-1})$ |
| **DM70** | 250 GeV | $\not{M} > 130$ GeV | $3\sigma$ $(3ab^{-1})$ |
| $\mathbf{DM55_{w95}}$ | 500 GeV | $\not{M} > 100$ GeV and $\not{M} < 150$ GeV | $3.6\sigma$ $(1ab^{-1})$ |
| **DM70** | 500 GeV | $\not{M} > 140$ GeV and $\not{M} < 190$ GeV | $1.5\sigma$ $(3ab^{-1})$ |
| $\mathbf{DM55_{w95}}$ | 1 TeV | $\not{M} > 120$ GeV and $\not{M} < 250$ GeV | $2.4\sigma$ $(3ab^{-1})$ |
| **DM70** | 1 TeV | $\not{M} > 120$ GeV and $\not{M} < 250$ GeV | $0.36\sigma$ $(3ab^{-1})$ |

**Lepton colliders a must to discover light DM in cases where LHC still hides it!**

## Intermediate DM

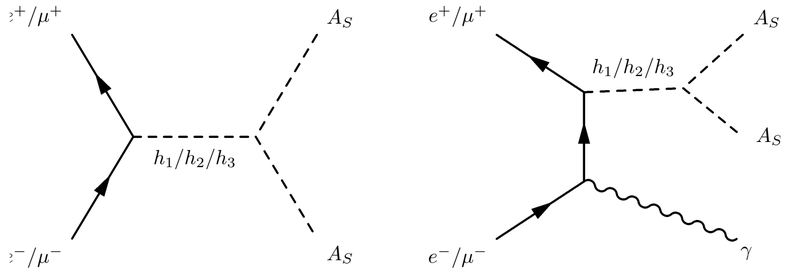
**Heavy and Intermediate DM benefit from associated production modes such as bbH and ttH at higher energy lepton colliders/proposed muon colliders.**

## bb + Missing Energy (3 and 10TeV muon collider)




| Benchmark | Cut | Significance |
|---|---|---|
| **DM156$_{w95}$** | 100 GeV $< m_{bb} <$ 500 GeV | $6.3\sigma$ $(3ab^{-1})$ |

| Benchmark | Cut | Significance |
|---|---|---|
| **DM156$_{w95}$** | 690 GeV $< \not{M} <$ 710 GeV | $3\sigma$ $(3ab^{-1})$, $5.3\sigma$ $(10ab^{-1})$ |

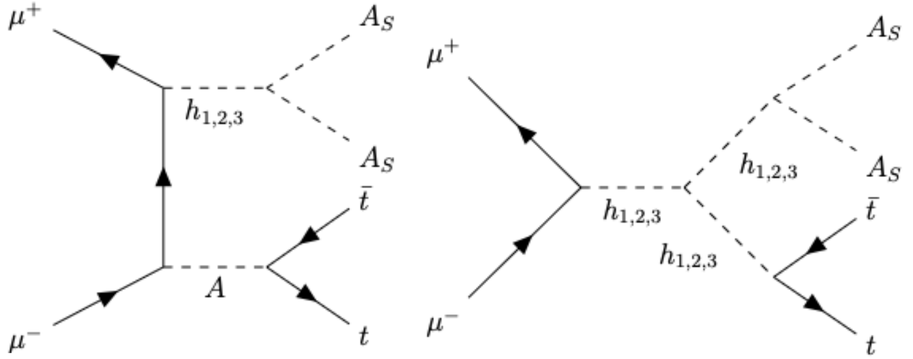



## Mono $\not{\gamma}$+ Missing Energy (1 TeV muon collider)

| Benchmark | Production cross-section (fb)at $\sqrt{s} = 1$ TeV |
|---|---|
| **DM156$_{w95}$** | 0.23 |
| $\nu\nu\gamma$ background | 2.45 |

| Cut | Significance |
|---|---|
| GeV $< \not{M} <$ 710 GeV | $3\sigma$ $(3ab^{-1})$, $5.3\sigma$ $(10ab^{-1})$ |

## Heavy DM

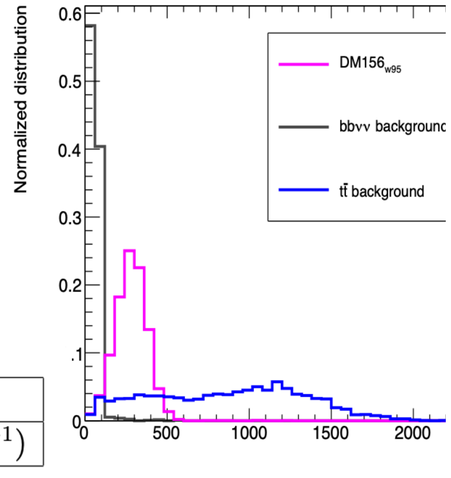


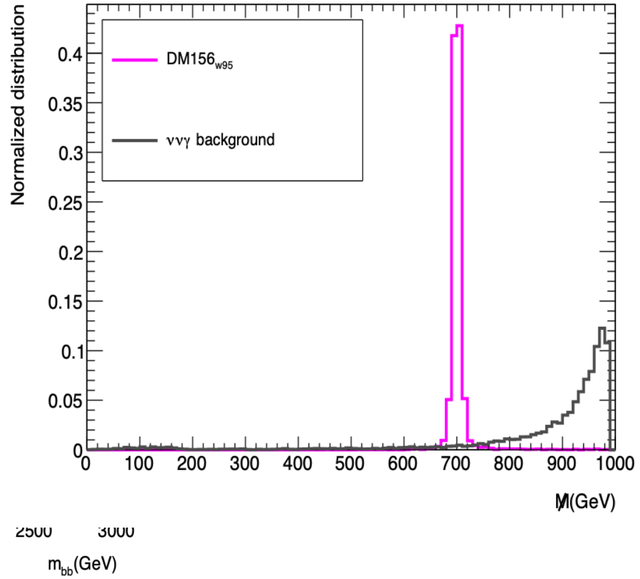

## tt + Missing Energy

## (10 TeV muon collider)

| Benchmark | Production cross-section (fb) at $\sqrt{s} = 10$ TeV |
|---|---|
| **DM1000$_{w95}$** | 0.027 |
| $t\bar{t}$+MET background | 1.66 |

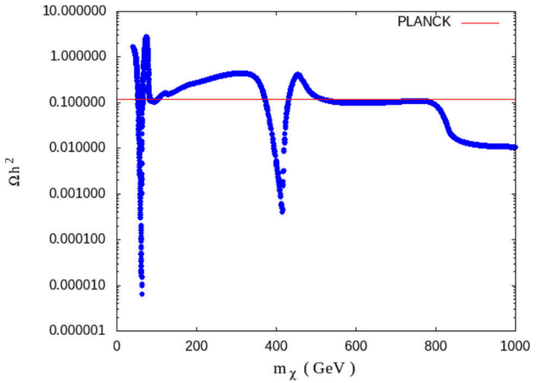
| Benchmark | Cut | Significance |
|---|---|---|
| **DM1000$_{w95}$** | $m_{bb} < 2$ TeV | $2.9\sigma$ $(10ab^{-1})$ |

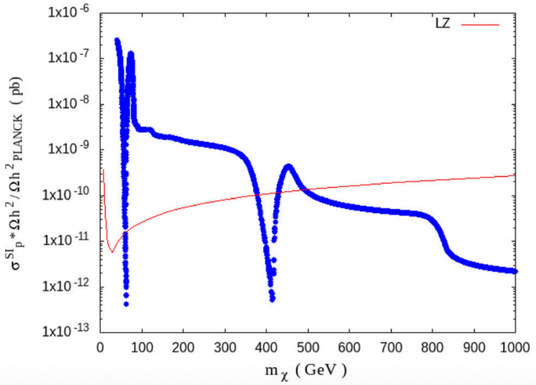


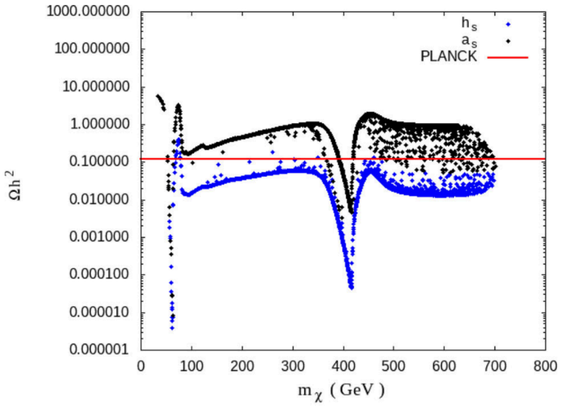



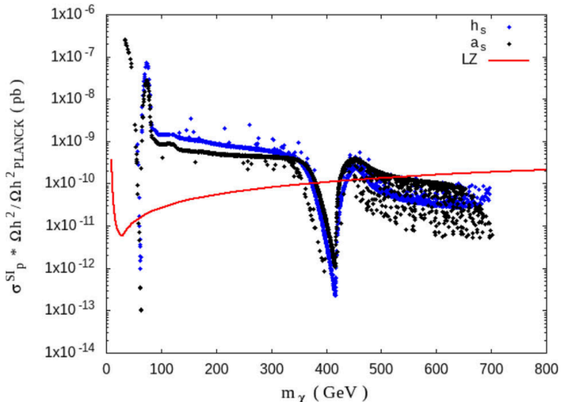
# Multicomponent DM in 2HDMS

| | $U(1)$ | $U(\not{1})$ |
|---|---|---|
| Free parameters | $m_S^{2'}, \lambda_1'', \lambda_4', \lambda_5' = 0$ | $m_S^{2'}, \lambda_1'', \lambda_4', \lambda_5' \neq 0$ |
| Mass of DM | $m_{h_s} = m_{a_s}$ | $m_{h_s} \neq m_{a_s}$ |
| DM candidates | $S$ | $h_s, a_s$ |



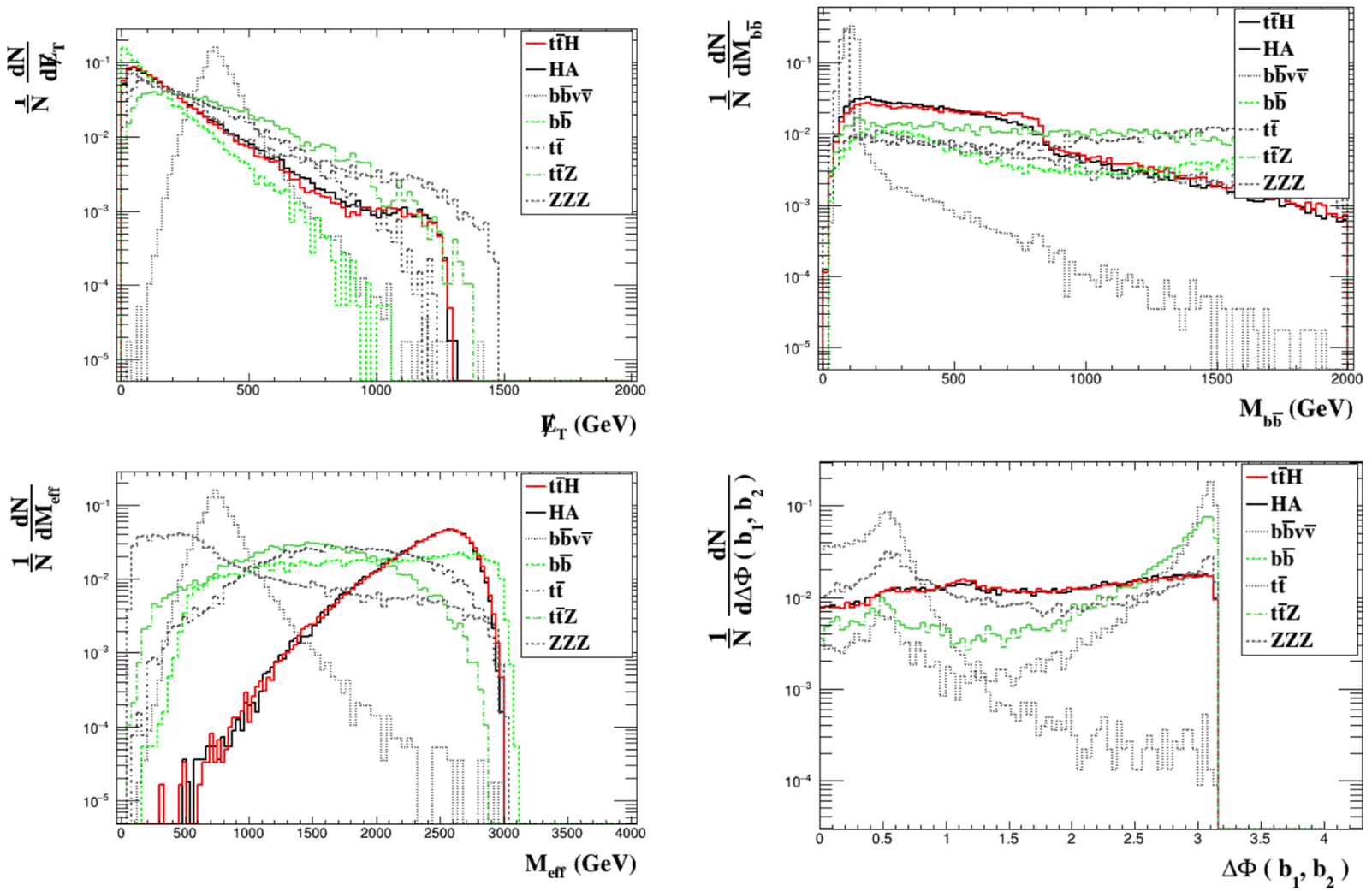




Eur.Phys.J.Plus 140 (2025) 1, 87

**For heavy DM, dominant contributions from ttH and HA in 2b + Missing Energy final states.**

$$e^- e^+ \to t\bar{t}H,\ HA$$




For heavy degenerate DM masses~400 GeV and Heavy Higgs mass ~ 833 GeV (with ~4% invisible branching)

signal significance of $\sim 2.74\sigma$ at an $e^+e^-$ collider at $\sqrt{s} = 3$ TeV at $5\text{ab}^{-1}$

**More detailed collider studies ongoing to explore full potential of multicomponent DM at higher energy linear colliders at 3 TeV!**

# Summary

- **Dark Matter remains one of the most challenging yet intriguing mysteries of Nature.**

- Extended Higgs portals models accommodating dark matter (such as the Type II 2HDM extended with a complex singlet scalar) very well motivated and **connect Particle Physics at low scale and the early Universe cosmology.**

- **Exciting signals which are hinted at HL-LHC, decisively detected at lepton colliders such as for light pseudoscalar DM at an $e^+e^-$ collider of 250 GeV via the Higgsstrahlung process using missing mass reconstruction techniques.**

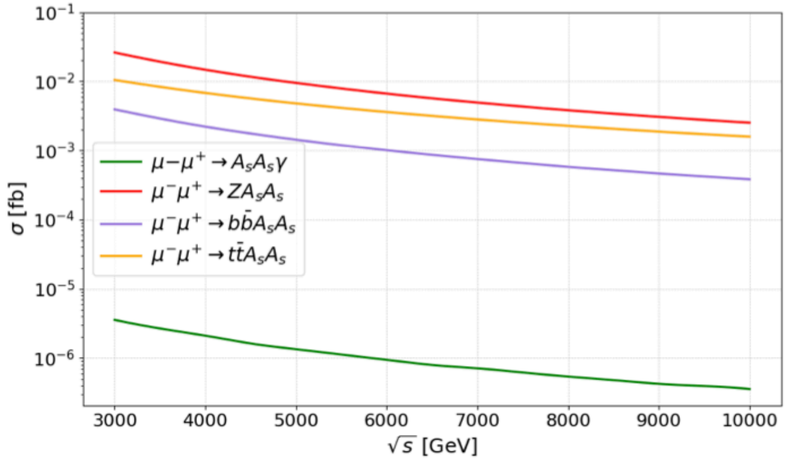
- **Associated production channels bbH, ttH, HA take over for heavy and intermediate DM cases at higher center of mass energies (~3 TeV) and beneficial to look for at higher energy lepton colliders akin to muon colliders to enhance reach of BSM higgs searches.**

- Potential for high energy lepton colliders to uncover **multi-component DM** at 3 TeV e+e- colliders for heavier DM masses.

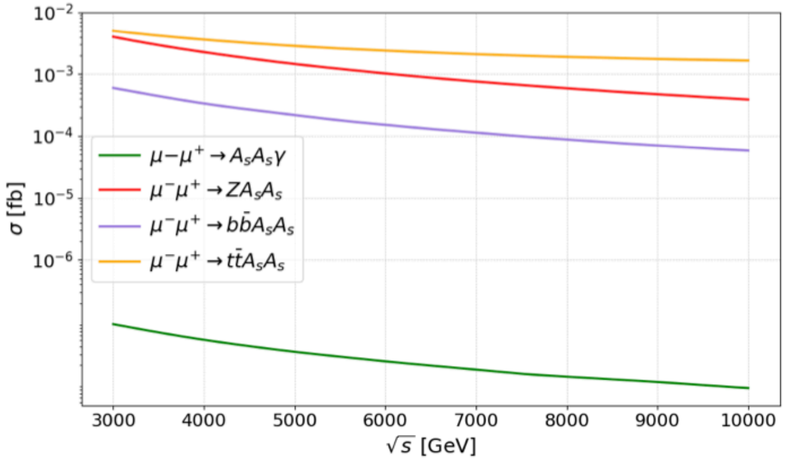
# Thank You

# At $\mu^+\mu^-$colliders:

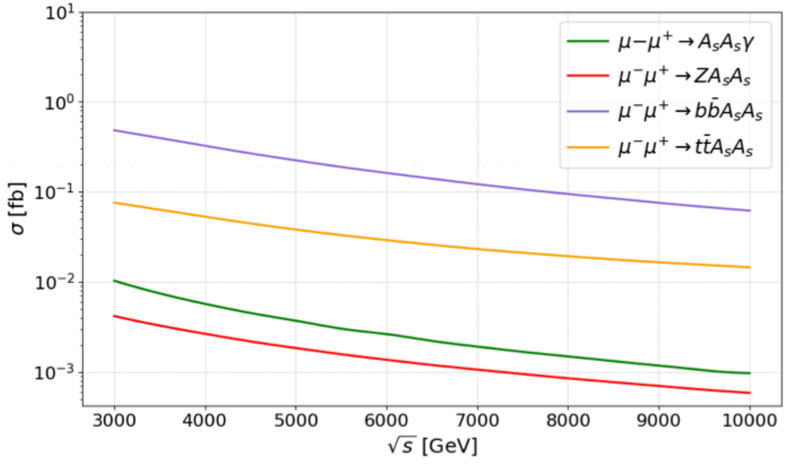
Relevant processes at muon colliders



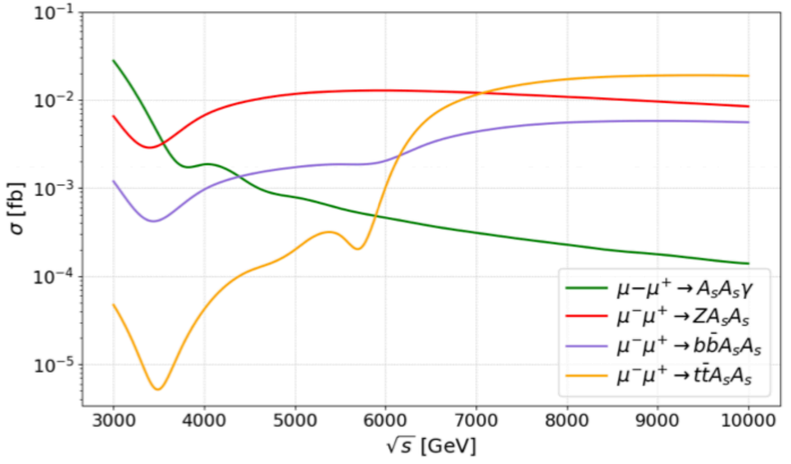

(a) $\mathbf{DM55_{w95}}$




(b) $\mathbf{DM70}$




(c) $\mathbf{DM156_{w95}}$




(d) $\mathbf{DM1000_{w95}}$

# Benchmarks

| $m_{h_1}$ | $m_{h_2}$ | $m_{h_3}$ | $m_A$ | $m_{H^\pm}$ | $\chi^2$ |
|---|---|---|---|---|---|
| 95.4 GeV | 125.09 GeV | 650 GeV | 800 GeV | 800 GeV | 1.26 |
| $m_{A_S}$ | $\lambda_1' - 2\lambda_4'$ | $\lambda_2' - 2\lambda_5'$ | $\lambda_1'' - \lambda_3''$ | $\tan\beta$ | |
| 55.596 GeV | 0.0020912 | 0.00074611 | −0.025735 | 2 | |
| $v_S$ | $\tilde{\mu}$ | $\alpha_1$ | $\alpha_2$ | $\alpha_3$ | |
| 300 GeV | 650 GeV | −1.932 | 1.272 | 1.484 | |

**DM55_w95**

| $m_{h_1}$ | $m_{h_2}$ | $m_{h_3}$ | $m_A$ | $m_{H^\pm}$ |
|---|---|---|---|---|
| 800 GeV | 125.09 GeV | 150 GeV | 800 GeV | 800 GeV |
| $m_{A_S}$ | $\lambda_1' - 2\lambda_4'$ | $\lambda_2' - 2\lambda_5'$ | $\lambda_1'' - \lambda_3''$ | $\tan\beta$ |
| 70 GeV | −0.10783 | 0.063127 | −0.47818 | 1.3728 |
| $v_S$ | $\tilde{\mu}$ | $\alpha_1$ | $\alpha_2$ | $\alpha_3$ |
| 219.05 GeV | 751.54 GeV | −0.60016 | 0.042445 | −0.054807 |

**DM70**

| $m_{h_1}$ | $m_{h_2}$ | $m_{h_3}$ | $m_A$ | $m_{H^\pm}$ | $\chi^2$ |
|---|---|---|---|---|---|
| 95.4 GeV | 125.09 GeV | 700 GeV | 700 GeV | 700 GeV | 0.422 |
| $m_{A_S}$ | $\lambda_1' - 2\lambda_4'$ | $\lambda_2' - 2\lambda_5'$ | $\lambda_1'' - \lambda_3''$ | $\tan\beta$ | |
| 156 GeV | 12.753 | −0.31351 | −2.6747 | 6.6 | |
| $v_S$ | $\tilde{\mu}$ | $\alpha_1$ | $\alpha_2$ | $\alpha_3$ | |
| 239.86 GeV | 700 GeV | 1.4661 | 1.1920 | −1.5989 | |

**DM156_w95**

| $m_{h_1}$ | $m_{h_2}$ | $m_{h_3}$ | $m_A$ | $m_{H^\pm}$ | $\chi^2$ |
|---|---|---|---|---|---|
| 95.4 GeV | 125.09 GeV | 2950 GeV | 2950 GeV | 2950 GeV | 2.13 |
| $m_{A_S}$ | $\lambda_1' - 2\lambda_4'$ | $\lambda_2' - 2\lambda_5'$ | $\lambda_1'' - \lambda_3''$ | $\tan\beta$ | |
| 1000 GeV | 21.231 | 0 | −1.4153 | 5 | |
| $v_S$ | $\tilde{\mu}$ | $\alpha_1$ | $\alpha_2$ | $\alpha_3$ | |
| 10005 GeV | 2949.29 GeV | −1.769 | 1.250 | 1.569 | |

**DM1000_w95**

# LHC Cross-sections

| Process | Production cross-section (fb) at $\sqrt{s} = 14$ TeV | | |
|---|---|---|---|
| | **DM55$_{\mathbf{w95}}$** | **DM156$_{\mathbf{w95}}$** | **DM70** |
| GGF($h_2 \to A_S A_S$) | 533.9 | - | $19.29\times10^3$ |
| GGF($h_3 \to A_S A_S$) | - | 0.015 | - |
| VBF($h_2 \to A_S A_S$) | 54.33 | - | $2.72\times10^3$ |
| VBF($h_3 \to A_S A_S$) | - | 0.134 | 0.0022 |
| BBH ($(b\bar{b}h_2 \to A_S A_S)$) | 21.6 | - | 0.137 |
| BBH ($(b\bar{b}h_3 \to A_S A_S)$) | - | 47.24 | - |

**Table 4**: The production cross-sections at leading order (LO) of the relevant processes at $\sqrt{s} = 14$ TeV at LHC. All cross-sections below $10^{-6}$ fb are denoted by '-'. For $b\bar{b}h_i$, with $i = 2, 3$, we use the Santander matched cross-section as defined in the text.

| Process | Production cross-section (fb) at $\sqrt{s} = 14$ TeV | | |
|---|---|---|---|
| | **DM400** | **DM1000** | **DM1000$_{\mathbf{w95}}$** |
| GGF($h_3 \to A_S A_S$) | 0.013 | $6.35\times10^{-7}$ | $4.5\times10^{-6}$ |
| VBF($h_3 \to A_S A_S$) | 0.0008 | - | - |
| BBH($h_3 \to A_S A_S$) | 0.007 | - | - |

| Benchmark | Production cross-section (fb) | |
|---|---|---|
| | at $\sqrt{s} = 3$ TeV | at $\sqrt{s} = 10$ TeV |
| **DM156$_{\mathbf{w95}}$** | 0.48 | 0.063 |
| $b\bar{b}\nu\nu$ background | 758 | 1.3 |
| $t\bar{t}$ background | 20 | 1.7 |

**bb+Missing Energy cross-sections at Muon Colliders.**

| Benchmark | Production cross-section (fb) | | |
|---|---|---|---|
| | at $\sqrt{s} = 250$ GeV | at $\sqrt{s} = 500$ GeV | at $\sqrt{s} = 1$ TeV |
| **DM55$_{\mathbf{w95}}$** | 4.42 | 1.1 | 0.24 |
| **DM70** | 0.33 | 0.15 | 0.035 |
| $\nu\bar{\nu}Z$ background | 503 | 491 | 950 |

**Mono Z + Missing energy cross-sections at Muon Colliders.**

| | $\Omega h^2$ | $\sigma_{\mathrm{p}A_S}$/pb | $\sigma_{\mathrm{n}A_S}$/pb | $\sigma_{A_SA_S\to XX}/\frac{\mathrm{cm}^3}{\mathrm{s}}$ | $BR(h_3 \to A_SA_S)$ | $BR(h_2 \to A_SA_S)$ |
|---|---|---|---|---|---|---|
| **DM55$_{\mathbf{w95}}$** | 0.11 | $4.21 \times 10^{-12}$ | $4.08 \times 10^{-12}$ | $1.98\times 10^{-28}$ | $3.81\times 10^{-9}$ | 0.0199 |
| **DM156$_{\mathbf{w95}}$** | $1.61 \times 10^{-4}$ | $3.903 \times 10^{-11}$ | $4.160 \times 10^{-11}$ | $3.875 \times 10^{-29}$ | 0.69 | - |
| **DM1000$_{\mathbf{w95}}$** | 0.111 | $3.323 \times 10^{-11}$ | $3.369\times 10^{-11}$ | $2.045\times 10^{-26}$ | 0.0359 | - |
| **DM70** | 0.113 | $8.938 \times 10^{-16}$ | $2.651\times 10^{-13}$ | $2.13\times 10^{-28}$ | 0.99934 | - |
| **DM400** | 0.106 | $4.960\times 10^{-11}$ | $5.101\times 10^{-11}$ | $3.67\times 10^{-26}$ | 0.82203 | - |
| **DM1000** | 0.117 | $8.263 \cdot 10^{-11}$ | $8.464 \cdot 10^{-11}$ | $2.018 \cdot 10^{-26}$ | 0.005 | - |

**Allowed Benchmarks**

# Couplings in 2HDM

The reduced Higgs to fermion couplings for all four Yukawa types are summarized in Tab. 1.

| | type I | type II | lepton-specific | flipped |
|---|---|---|---|---|
| $c_{h_i tt}$ | $\frac{R_{i2}}{\sin\beta}$ | $\frac{R_{i2}}{\sin\beta}$ | $\frac{R_{i2}}{\sin\beta}$ | $\frac{R_{i2}}{\sin\beta}$ |
| $c_{h_i bb}$ | $\frac{R_{i2}}{\sin\beta}$ | $\frac{R_{i1}}{\cos\beta}$ | $\frac{R_{i2}}{\sin\beta}$ | $\frac{R_{i1}}{\cos\beta}$ |
| $c_{h_i \tau\tau}$ | $\frac{R_{i2}}{\sin\beta}$ | $\frac{R_{i1}}{\cos\beta}$ | $\frac{R_{i1}}{\cos\beta}$ | $\frac{R_{i2}}{\sin\beta}$ |

**Table 1:** Higgs to fermion reduced couplings for different type of Yukawa couplings

**Gauge couplings in 2HDM**

$$c_{h_i VV} = c_{h_i ZZ} = c_{h_i WW} = \cos\beta R_{i1} + \sin\beta R_{i2}$$

**Rotation Matrix**

$$R = \begin{pmatrix} c_{\alpha_1}c_{\alpha_2} & s_{\alpha_1}c_{\alpha_2} & s_{\alpha_2} \\ -s_{\alpha_1}c_{\alpha_3} - c_{\alpha_1}s_{\alpha_2}s_{\alpha_3} & c_{\alpha_1}c_{\alpha_3} - s_{\alpha_1}s_{\alpha_2}s_{\alpha_3} & c_{\alpha_2}s_{\alpha_3} \\ s_{\alpha_1}s_{\alpha_3} - c_{\alpha_1}s_{\alpha_2}c_{\alpha_3} & -c_{\alpha_1}s_{\alpha_3} - s_{\alpha_1}s_{\alpha_2}c_{\alpha_3} & c_{\alpha_2}c_{\alpha_3} \end{pmatrix}$$

Branco, et.al,
https://doi.org/10.1016/j.physrep.2012.02.002

# Benchmark

| Parameters | **BP3** |
|---|---|
| $\lambda_1$ | 0.21 |
| $\lambda_2$ | 0.26 |
| $\lambda_3$ | 0.25 |
| $\lambda_4$ | –0.1 |
| $\lambda_5$ | 0.1 |
| $\lambda_1^{''m}$ | 0.01 |
| $\lambda_2^{''m}$ | 0.0001 |
| $\lambda_3^{''m}$ | 0.001 |
| $\lambda_1^{'m}$ | 2.0 |
| $\lambda_2^{'m}$ | 0.1 |
| $\lambda_4^{'m}$ | –0.1 |
| $\lambda_5^{'m}$ | -0.1 |
| $m_{12}^2(\text{GeV}^2)$ | $1.0\times10^5$ |
| $m_{DM_1}^2(\text{GeV}^2)$ | 300000 |
| $m_{DM_2}^2(\text{GeV}^2)$ | 380000 |
| $\tan\beta$ | 6.8 |
| $\cos(\alpha-\beta)$ | –0.00015 |
| $m_h$ (GeV) | 125.6 |
| $m_H$(GeV) | 833.5 |
| $m_A$(GeV) | 829.8 |
| $m_{H^\pm}$ (GeV) | 833.5 |
| $m_{a_s}$ (GeV) | 398.12 |
| $m_{h_s}$ (GeV) | 428.88 |
| BR($H\to a_s a_s$) | $3.9\times10^{-2}$ |
| $\Omega h^2$ | $1.03\times10^{-3}$ |
| $\sigma_p^{SI} * \frac{\Omega h^2}{\Omega h^2_{PLANCK}}$ ($\times10^{11}$ pb) | 2.66 |
| $\sigma_n^{SI} * \frac{\Omega h^2}{\Omega h^2_{PLANCK}}$ ($\times10^{11}$ pb) | 2.79 |

# Backgrounds and cuts for multicomponent DM

We study the final state of $2b+\not{E}_T$ with the missing energy arising from $H \to \chi\bar{\chi}$ at an unpolarized $e^+e^-$ collider for an integrated luminosity of $\mathcal{L} = 5$ ab$^{-1}$. Dominant SM background contributions arise from

- $b\bar{b}$ (for misidentification of decay products of $b$-quark along with missing energy from $b$ decays)
- $b\bar{b}\nu\bar{\nu}$ (including both on-shell and off-shell contribution from $Z$ boson decay as well as $\nu\bar{\nu}h$ contribution)
- $Z(\to b\bar{b})Z(\to \nu\bar{\nu})$
- $hZ$ ($h \to b\bar{b}$, $Z \to \nu\bar{\nu}$)
- $t\bar{t}Z$, ($Z \to \nu\bar{\nu}$, $t \to bW^+$) for misidentified leptons/jets from $W$ bosons.
- Leptonic $t\bar{t}$ for misidentified leptons or semi-leptonic $t\bar{t}$ decays with missing energy arising from the $b$ decaying leptonically.
- $WWZ$
- $ZZZ$

**Cuts for analysis: 2b + MET**

- **C1**: The final state consists of two b-jets and no leptons or photons.
- **C2**: The leading b-jet has transverse momentum $p_T > 100$ GeV and sub-leading b-jet has $p_T > 80$ GeV. The hard $p_T$ cuts on the b-jets help to reduce backgrounds from SM backgrounds from $Z$ and $h$ bosons.
- **C3**: The invariant mass of the two b-jets within the mass window 80 GeV $< M_{b_1\, b_2} <$130 GeV is rejected to remove contributions from $Z$ and $h$ bosons.

- **C4**: Since the dark matter is heavy, we demand a large cut on the effective mass $M_{eff} > 1.2$ TeV where $M_{eff} = \sum_i (p_{T_i}) + \not{E}_T$.
- **C5**: Further, we demand $\not{E}_T > 650$ GeV on the final state which reduces the dominant SM backgrounds.
- **C6**: The $\Delta\Phi$ between two b-jets is significantly different for the signal and background from $b\bar{b}$ where the b-jets are mostly back-to-back. We demand $\Delta\Phi(b_1, b_2) < 1.60$. This also reduces the backgrounds from $b\bar{b}$ as well as from $t\bar{t}$ and $t\bar{t}Z$ sharply.